MADRID
inter.noise 2019
June 16 - 19
NOISE CONTROL FOR A BETTER ENVIRONMENT

Modeling one-dimensional phononic crystal rods using a state space formulation

Lima, Vinícius Dias [1]
School of Mechanical Engineering University of Campinas
Rua Mendeleyev, 200, Campinas, SP, Brazil

Beli, Danilo[2]
School of Mechanical Engineering University of Campinas
Rua Mendeleyev, 200, Campinas, SP, Brazil

Arruda, José Roberto F.[3]
School of Mechanical Engineering University of Campinas
Rua Mendeleyev, 200, Campinas, SP, Brazil

ABSTRACT

Phononic crystals are periodic structures wherein elastic waves propagate. Due to Bragg scattering, periodicity creates frequency bands where waves become evanescent and standing wave modes cannot build up (band gaps). This property can be used for vibration and noise control. The plane wave expansion (PWE) method is the most commonly used method to obtain the dispersion diagram from the periodic cell properties by imposing the Bloch-Floquet periodicity (infinite structure behavior). However, it does not compute the forced response of a finite structure. Spectral elements are an efficient way to represent analytically the dynamic stiffness matrix of a periodic cell. However, spectral elements are available only for uniform or tapered cells, or combinations of those. Otherwise, a finite element model of the cell can be used. In this work, a modeling technique that can be used to compute the band diagram and the forced response of one-dimensional phononic crystals with spatially varying elastic and geometrical properties is presented. The technique consists of transforming the equations of motion, a boundary value problem, into a spectral (harmonic) spatial domain initial value problem in state-space form. By transforming the state variables to mechanical impedance variables produces a Riccati equation, which can be numerically integrated starting from a waveguide end, as the impedance value can be known from the boundary conditions. Solving the Riccati equation allows computing

[1] vinidiaslima@gmail.com
[2] dbeli@fem.unicamp.br
[3] arruda@fem.unicamp.br

the transfer matrix and, from it, the dynamic stiffness matrix. This formulation can be used for one-dimensional elastic waveguides such as rods, acoustic ducts, beams, and Levy plates. Numerical examples of rods are presented. The method is computationally efficient and presents good convergence properties. In this work the shape of a periodic rod with varying cross-sectional area is designed for a low frequency and broad first band gap and the forced response is computed using the state space formulation. Experimental results are also presented.

Keywords: Periodic structure, band gap, phononic crystal,state-space,Riccati
I-INCE Classification of Subject Number: 43
(see http://i-ince.org/files/data/classification.pdf)

1. INTRODUCTION

Phononic crystals are periodic structures which exhibit band gaps in their dispersion diagram due to Bragg scattering [1, 2]. In this work, we are interested in their use for vibration and sound attenuation [3, 4]. These elastic systems are usually modeled as boundary value problems in the spatial domain and as initial value problems in the time domain. The resulting equations of motion can be solved by analytical or numerical approaches [5]. The dispersion diagrams can be obtained from the homogeneous equations of motion applying the Bloch-Floquet periodic condition on the displacement field [6]. The plane wave expansion (PWE) method is the most widely used. It expresses the periodic material and geometrical properties as a spatial domain Fourier series expansion [7]. An alternative analytical technique consists of using a spectral element model.

For spatially varying properties, SEM elements exist only for simple cases, such as linearly/tapered or exponential distributions [8, 9]. For arbitrarily shaped waveguides, a stepped SEM can be used, but this approach can present numerical issues [10]. In this work, the second order partial differential elastodynamic equation of an arbitrarily shaped rod is written as a first order system of equations. This space-state formulation transforms the boundary value problem into an initial value problem [11]. However, as only the relation between the forces and displacements is known in a boundary value problem, the system of equations is rewritten in terms of the mechanical impedance [12]. The transformed equation is shown to be a Riccati differential equation in the spatial domain with varying properties. The impedance is known in a boundary value problem and, therefore, the Riccati equation can be solved. This method originally used to compute the mechanical impedance of a beam with varying thickness [13].

Given the impedance at the two ends of a periodic rod cell, this work shows how to obtain the transfer matrix and the dynamic stiffness matrix of the rod element with arbitrary shape. This can be interpreted as a spectral element with arbitrary shape. This spectral element is used to compute the forced response of arbitrarily shaped phononic crystal rods. The shape of the rod cell can be optimized using the Fourier coefficients in the PWE method, while the forced response of a structure composed of the periodic rod cells can be computed with the proposed state-space/Riccati approach. The proposed method can be extended to treat many types of one-dimensional elastic waveguides, such as beams, acoustic ducts, and Levy plates [14].

2. FORMULATION

In this section the plane wave expansion method is applied to a simple rod with varying cross-sectional area expanded in Fourier series. The PWE can be found in the literature, but we present it for this simple case aiming at introducing the topic to the noise control engineering community and facilitating the involvement of neophytes with the phononic crystal concept.

2.2.1. Plane wave expansion for rods

The wave equation for an elastic rod with varying cross-sectional area can be written as:

$$\frac{\partial}{\partial x}\left(ES(x)\frac{\partial u(x,t)}{\partial x}\right) = \rho S(x)\frac{\partial^2 u(x,t)}{\partial t^2} \tag{1}$$

Here the Young's modulus E and the specific mass ρ are assumed constant, but they might also vary along the rod. Thus, the dependence upon x is expressed in S and u and omitted in E and ρ.

Applying the Fourier transform in Equation 1 yields:

$$\frac{\partial}{\partial x}\left(ES(x)\frac{\partial u(x,\omega)}{\partial x}\right) = -\omega^2\rho S(x)u(x,\omega) \tag{2}$$

From the Bloch-Floquet theorem, the Bloch wave function for the displacement $u(x,\omega)$ is given by:

$$u(x,\omega) = e^{jkx}u_k(x,\omega) \tag{3}$$

where the $u_k(x,\omega)$ is the amplitude function of a wave in one cell, or Bloch wave amplitude, dependent of the wave number k. Expanding it as a Fourier series in the reciprocal space (wavenumber domain) of the dimension x results in:

$$u(x,\omega) = e^{jkx}\sum_{n=-\infty}^{+\infty}\hat{u}_k(g,\omega)e^{jgx} = \sum_{n=-\infty}^{+\infty}\hat{u}_k(g,\omega)e^{j(k+g)x} \tag{4}$$

where $g = 2\pi n/a$, a is the cell length and $n \in \mathbb{Z}$. The expansion of the cross sectional area as a Fourier series results in:

$$S(x) = \sum_{\bar{n}=-\infty}^{+\infty}\hat{S}(\bar{g})e^{j\bar{g}x} \tag{5}$$

where $\bar{g} = 2\pi\bar{n}/a$ with $\bar{n} \in \mathbb{Z}$.

The term on the right side of Equation 2 can be rewritten using Equations. 4 and 5:

$$\omega^2\rho S(x)u(x,\omega) = \sum_{n=-\infty}^{+\infty}\sum_{\bar{n}=-\infty}^{+\infty}\omega^2\rho\hat{S}(\bar{g})\hat{u}_k(g,\omega)e^{j(k+g+\bar{g})x} \tag{6}$$

Denoting $\breve{g} = \bar{g} + g$ and substituting in Equation 6 yields:

$$\omega^2\rho S(x)u(x,\omega) = \sum_{n=-\infty}^{+\infty}\sum_{\breve{n}=-\infty}^{+\infty}\omega^2\rho\hat{S}(\breve{g}-g)\hat{u}_k(g,\omega)e^{j(k+\breve{g})x} \tag{7}$$

where $\breve{g} = 2\pi\breve{n}/a$ with $\breve{n} \in \mathbb{Z}$. Similarly, the left term can be obtained as

$$\frac{\partial}{\partial x}\left[ES(x)\frac{\partial u(x,\omega)}{\partial x}\right] = -\sum_{g=-\infty}^{+\infty}\sum_{\breve{g}=-\infty}^{+\infty} E\hat{S}(\breve{g}-g)\hat{u}_k(g,\omega)(k+g)(k+\breve{g})e^{j(k+\breve{g})x} \tag{8}$$

Hence, Equation 2 may be rewritten as:

$$\begin{aligned}\Bigg[\sum_{g=-\infty}^{+\infty}\sum_{\breve{g}=-\infty}^{+\infty} E\hat{S}(\breve{g}-g)\hat{u}_k(g,\omega)(k+g)(k+\breve{g})e^{j\breve{g}x} \\ -\sum_{g=-\infty}^{+\infty}\sum_{\breve{g}=-\infty}^{+\infty}\omega^2\rho\hat{S}(\breve{g}-g)\hat{u}_k(g,\omega)e^{j\breve{g}x}\Bigg]e^{jkx} = 0\end{aligned} \tag{9}$$

Multiplying Equation 9 by $e^{-j\bar{g}x}$ and integrating over the unit-cell length for $e^{-jkx} \neq 0$ yields:

$$\begin{aligned}\sum_{g=-\infty}^{+\infty}\sum_{\breve{g}=-\infty}^{+\infty} E\hat{S}(\breve{g}-g)\hat{u}_k(g,\omega)(k+g)(k+\breve{g})\frac{1}{h}\int e^{j(\breve{g}-\bar{g})x}dx \\ -\sum_{g=-\infty}^{+\infty}\sum_{\breve{g}=-\infty}^{+\infty}\omega^2\rho\hat{S}(\breve{g}-g)\hat{u}_k(g,\omega)\frac{1}{h}\int e^{j(\breve{g}-\bar{g})x}dx = 0\end{aligned} \tag{10}$$

Recalling that

$$\frac{1}{h}\int e^{j(\breve{g}-\bar{g})x}dx = \delta_{\breve{g}\bar{g}} \tag{11}$$

where $\delta_{\breve{g}\bar{g}}$ is the Kronecker delta, which is non-zero only when $\breve{g} = \bar{g}$. Equation 10 can be simplified and rearranged as:

$$\sum_{g=-\infty}^{+\infty}\omega^2\rho\hat{S}(\bar{g}-g)\hat{u}_k(g,\omega) = \sum_{g=-\infty}^{+\infty} E\hat{S}(\bar{g}-g)(k+g)(k+\bar{g})\hat{u}_k(g,\omega) \tag{12}$$

Truncating the summation with $g, \bar{g} = [-N, N]$ results in $2N+1$ coefficients and Equation 12 can be written as:

$$\omega^2\sum_{g=-N}^{+N}\rho\hat{S}(\bar{g}-g)\hat{u}_k(g,\omega) = \sum_{g=-N}^{+N} E\hat{S}(\bar{g}-g)(k+g)(k+\bar{g})\hat{u}_k(g,\omega) \tag{13}$$

Equation 13 can be written in matrix form as:

$$\boldsymbol{A}(k)U(g) = \omega^2\boldsymbol{B}(k)U(g) \tag{14}$$

where $U(g) = u_k(g,\omega)$. The elements of the $(2N+1)\times(2N+1)$ matrices $\boldsymbol{A}$ and $\boldsymbol{B}$ are defined as

$$\begin{aligned}\boldsymbol{A}_{ij}(k) = E\hat{S}(\bar{g}_i - g_j)(k+g_j)(k+\bar{g}_i) \\ \boldsymbol{B}_{ij}(k) = \rho\hat{S}(\bar{g}_i - g_j)\end{aligned} \tag{15}$$

where $\bar{g}_i = 2\pi i/a$ and $g_j = 2\pi j/a$ with $i, j = [-N, N]$. Equation 14 represents the generalized eigenvalue problem that should be solved for wave numbers within the irreducible Brillouin zone $ka/\pi = [0, 1]$. When the wavenumber is zero or π the term e^{ikx} has a unitary magnitude and thus there is no propagation. In this case, it can be shown that k has an imaginary part, which implies that waves decay along x. Such

non-propagating waves are called evanescent waves. In the frequency ranges where this happens there is no propagation and, therefore, there can be no standing waves and, thus, no vibration modes. Furthermore, because of the decay, vibration will be attenuated along x in this frequency range, denominated band gap or stop band. The easiest way to visualize band gaps is plotting $k(\omega)$ or $\omega(k)$, which is referred to as dispersion diagram.

2.2.2. Space state formulation for rods

In this section the elastodynamic equation in the frequency domain is written in state-space form. A coordinate transformation yields a Riccati differential equation, which can be solved given the boundary conditions. It is shown how to derive the transfer matrix and the dynamic stiffness matrix of an arbitrarily shaped rod element. Knowing the expression for the internal longitudinal force in a rod, $\hat{q}(x) = ES(x)\frac{\partial \hat{u}(x)}{\partial x}$, Equation 2 can be written as a system of first order partial differential equation, i.e. the state space form:

$$\frac{\partial \hat{q}(x)}{\partial x} = -\rho S(x)\omega^2 \hat{u}(x) \frac{\partial \hat{u}(x)}{\partial x} = \frac{\hat{q}(x)}{EA(x)} \tag{16}$$

which can be written in matrix form as:

$$\frac{\partial \hat{p}}{\partial x} = \mathbf{H}\hat{p} \tag{17}$$

with the state $\hat{p}(x) := \hat{p}(x, \omega)$ and the system matrix $\mathbf{H}(x, \omega)$ given by:

$$\hat{p}(x) = \begin{bmatrix} \hat{u}(x) \\ \hat{q}(x) \end{bmatrix} \qquad \text{and} \qquad \mathbf{H}(x,\omega) = \begin{bmatrix} \mathbf{H}_{11} & \mathbf{H}_{12} \\ \mathbf{H}_{21} & \mathbf{H}_{22} \end{bmatrix} = \begin{bmatrix} 0 & \frac{1}{ES(x)} \\ -\rho S(x)\omega^2 & 0 \end{bmatrix} \tag{18}$$

It is straightforward to solve Equation 17 numerically for any type of variation of the parameters along x. However, the initial state cannot be known, as the boundary condition is either of the force (Neumann) the displacement (Dirichlet), or mixed (force/displacement relation); the other variable of the state being unknown. To overcome this issue, one can rewrite the problem in terms of the mechanical impedance $\hat{z}(x)$, which is a relation between the state variables. For any boundary condition, the relation between the state variables and, hence, the impedance is known. Therefore, a coordinate transformation is necessary [13]:

$$\hat{q}(x) = i\omega \hat{z}(x)\hat{u}(x) \tag{19}$$

Substituting Equation 19 in Equation 17, one obtains the following set of equations:

$$\frac{\partial \hat{u}(x)}{\partial x} = \mathbf{H}_{11}\hat{u}(x) + \mathbf{H}_{12}\hat{q}(x) \qquad \text{and} \qquad i\omega \frac{\partial \hat{z}(x)\hat{u}(x)}{\partial x} = \mathbf{H}_{21}\hat{u}(x) + \mathbf{H}_{22}\hat{q}(x) \tag{20}$$

which lead to:

$$i\omega\left(\frac{\partial \hat{z}(x)}{\partial x}\hat{u}(x) + \hat{z}(x)\mathbf{H}_{11}\hat{u}(x) + \hat{z}(x)\mathbf{H}_{12}i\omega\hat{z}\hat{u}(x)\right) = \mathbf{H}_{21}\hat{u}(x) + \mathbf{H}_{22}i\omega\hat{z}(x)\hat{u}(x) \tag{21}$$

Since $\hat{u}(x)$ cannot be identically zero, one finally obtains the following Riccati type equation:

$$\frac{\partial \hat{z}(x)}{\partial x} + \hat{z}(x)\mathbf{H}_{11} - \mathbf{H}_{22}\hat{z}(x) + i\omega\hat{z}(x)\mathbf{H}_{12}\hat{z}(x) = (i\omega)^{-1}\mathbf{H}_{21} \tag{22}$$

For this equation, an initial condition $\hat{z}(0) = 0$ can be used for a free end, where $\hat{q}_0 = 0$ and $\hat{u}_0$ is unknown, but not zero.

After evaluating $\hat{z}(x = L)$ by integrating the Riccati equation, one can consider a unitary external force $\hat{q}(x = L) = 1$. Equation 19 can be used to compute the displacement. With the state at $x = L$ known, and using it as a initial condition in Equation 17, the state at $x = 0$ is obtained by integration of the state equations. Then, the full state at both ends allows computing the transfer matrix, since it relates the state at the two ends of the free-free finite rod.

$$\hat{p}(L) = \hat{T}(\omega)\hat{p}(0) \tag{23}$$

where $\hat{T}$ is the $[2 \times 2]$ transfer matrix. Applying the boundary conditions $\hat{q}(x = L) = 1$ and $\hat{q}(x = 0) = 0$ leads to

$$\begin{Bmatrix} \hat{u}_L \\ 1 \end{Bmatrix} = \begin{bmatrix} T_{11} & T_{12} \\ T_{21} & T_{22} \end{bmatrix} \begin{Bmatrix} \hat{u}_0 \\ 0 \end{Bmatrix} \tag{24}$$

Solving this algebraic system of equations leads to

$$\begin{cases} T_{11} = \hat{u}_L/\hat{u}_0 \\ T_{21} = \hat{u}_0^{-1} \end{cases} \tag{25}$$

In order to obtain T_{12} and T_{22}, the initial condition is applied at the other end, $x = L$ and the impedance is integrated in the opposite direction up to $x = 0$. Repeating the procedure done earlier, we have $\hat{p}(0)$ and $\hat{p}(L)$. Applying the new boundary conditions: $\hat{q}(x = L) =$ and $\hat{q}(x = 0) = 1$, the transfer matrix relation becomes:

$$\begin{Bmatrix} \hat{u}_L \\ 0 \end{Bmatrix} = \begin{bmatrix} T_{11} & T_{12} \\ T_{21} & T_{22} \end{bmatrix} \begin{Bmatrix} \hat{u}_0 \\ 1 \end{Bmatrix} \tag{26}$$

Without loss of generality we consider now a rod symmetric with respect to its center $x = L/2$. In this case we can write T_{12} and T_{22} in terms of T_{11} andT_{21}:

$$\begin{cases} T_{12} = (T_{11}^2 - 1)T_{21}^{-1} \\ T_{22} = T_{11} \end{cases} \tag{27}$$

The transfer matrix and, consequently, the dynamic stiffness matrix, are obtained. The stiffness matrix can be written as:

$$\begin{bmatrix} K_{11} & K_{12} \\ K_{21} & K_{22} \end{bmatrix} = \begin{bmatrix} T_{12}^{-1}T_{11} & -T_{12}^{-1} \\ T_{21} - T_{22}T_{12}^{-1}T_{11} & T_{22}T_{12}^{-1} \end{bmatrix} \tag{28}$$

For a periodic rod, the periodic cell dynamic stiffness matrix is computed as explained above, and a global dynamic stiffness matrix is assembled for a given number of rod cells. With the global matrix the forced responses can be easily computed. The proposed method can be seen as a method to derive the spectral element matrix of a structure with arbitrarily varying properties along its length.

3. NUMERICAL RESULTS

To illustrate the proposed method, we treat a simple example of a rod consisting of three identical cells along its length. The axisymmetric rod cell is shaped using semicircles of radius $r_c = a/4$ and a minimum radius of $r_{min} = 0.01m$ as shown in Figure 1. The material and geometrical properties are shown in Table 1.

Given the expression of the radius along the cell length $x = [-a/2, a/2]$:

$$\begin{aligned} r(x) &= r_{min} + r_c - \sqrt{r_c^2 - (2r_c - x)^2}, \quad -a/2 < x - a/4 \\ r(x) &= r_{min} + r_c + \sqrt{r_c^2 - x^2}, \quad -a/4 < x < a/4 \\ r(x) &= r_{min} + r_c - \sqrt{r_c^2 - (x - 2r_c)^2}, \quad a/4 < x < a/2 \end{aligned} \tag{29}$$

one can compute the cross-sectional area as a function of position x.

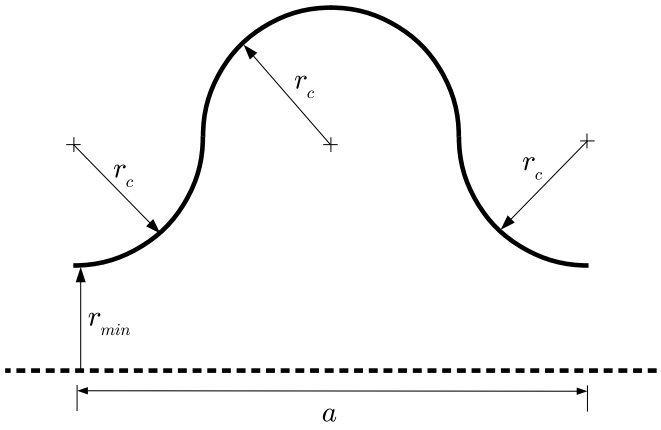

Figure 1: Unit rod cell geometry (axisymmetric).

Table 1: Material and geometrical properties fo the rod

Material property	Symbol	Value	Units
Young's modulus	E	81.5×10^9	N/m^2
Mass density	ρ	8600	kg/m^3
Cell length	a	0.06	m
Minimum radius	r_{min}	0.008	m
Profile radius	r_c	$a/4$	m

Given the cross-sectional area as a function of x one can obtain the Fourier series coefficients using the Discrete Fourier Transform (DFT). Here we have used 7397 points along x. Given that the shape is symmetrical with respect to $x = 0$, i.e. an even function, the Fourier series coefficients are real and the Fourier series is also an even function. Therefore only half the Fourier series coefficients are necessary to define the cross-sectional area.

Applying the PWE method exposed in Section 2.1 the dispersion diagram shown in Figure 2 is obtained. A large band gap opens at 8950 Hz. It closes at 48 kHz. The PWE method is a straightforward way to obtain the dispersion diagram. Otherwise, the eigenvalues of the transfer matrix also give the wavenumbers (as a consequence of the Bloch-Floquet theorem). The latter give not only the real part of the wavenumber, but also its imaginary part. A dispersion diagram with the real part in the positive axis and the imaginary part in the negative axis (standard way of depicting the dispersion diagram) obtained from the eigenvalues of the transfer matrix obtained using the state-space/Riccati method of Section 2.2 is shown for a larger frequency range in Figure 3.

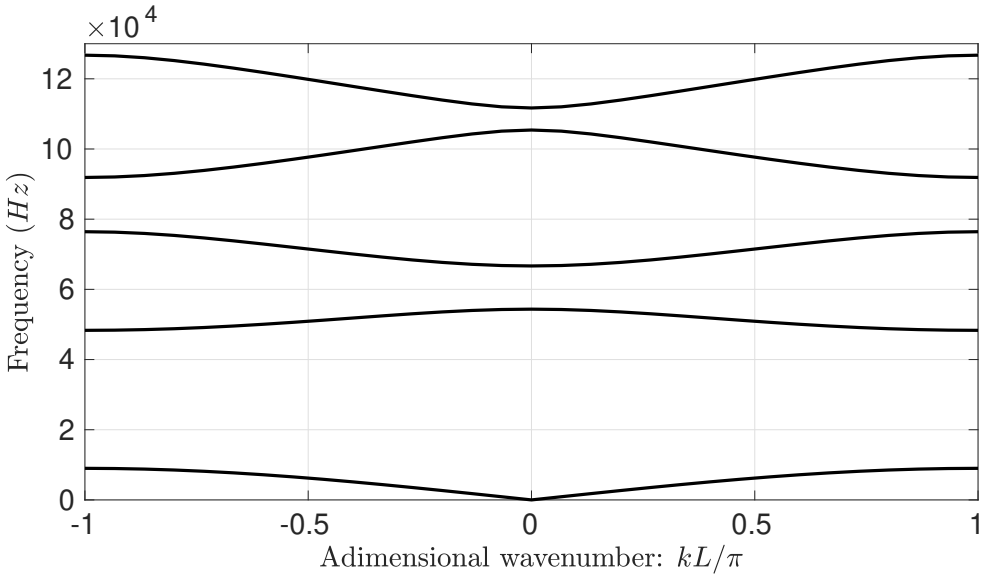

Figure 2: Dispersion diagram computed using the PWE method.

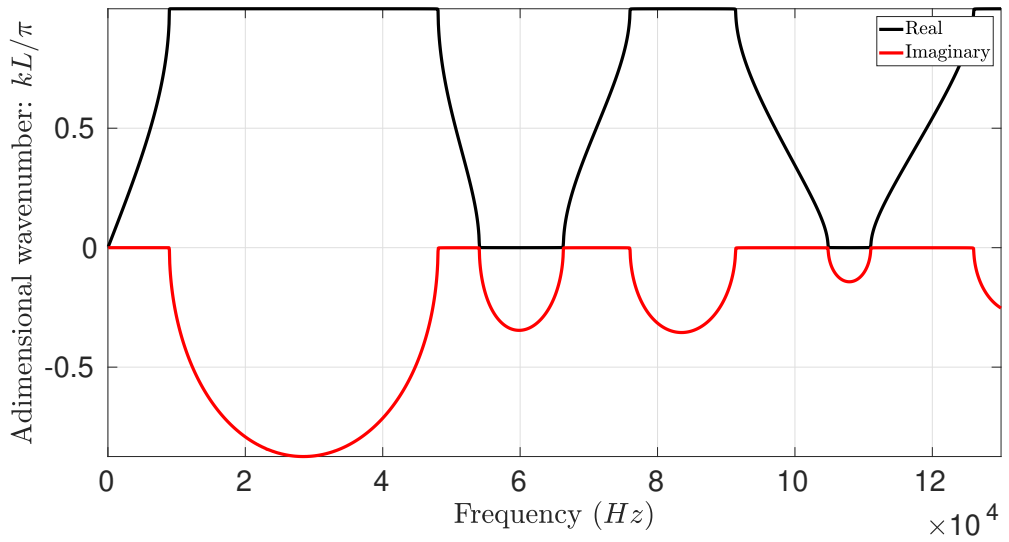

Figure 3: Dispersion diagram computed using the eigenvalues of the transfer matrix.

To compute the forced response the state-space/Riccati method of Section 2.2 was used to derive the spectral element of one cell and the global stiffness matrix was assembled for three cells (using the direct stiffness method commonly used in finite

element models). Applying a unit force at one end the acceleration response at the other end can be computed for each frequency, which is the Frequency Response Function (FRF). Figure 4 shows the computed FRF.

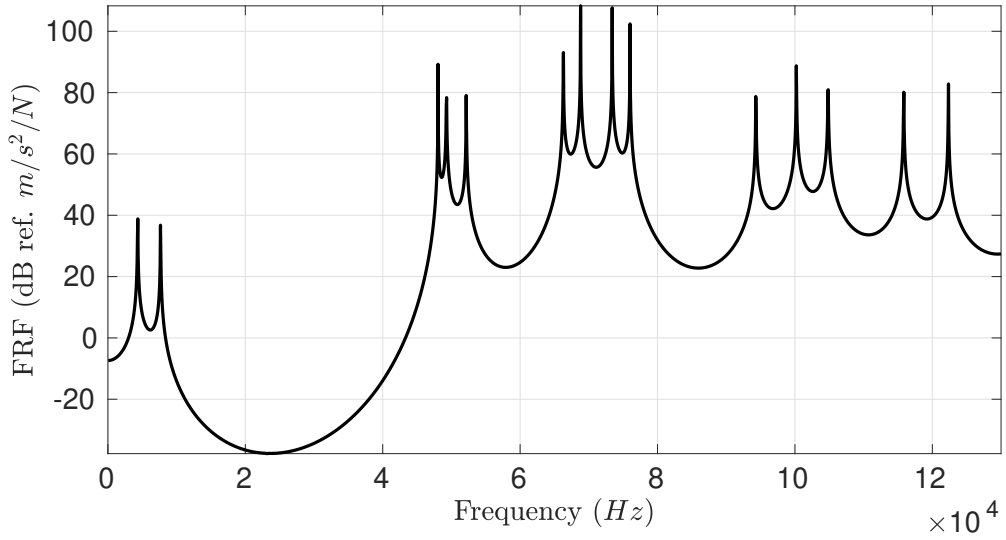

Figure 4: FRF for a free-free three-cell rod with excitation at one end and response at the other end.

4. EXPERIMENTAL RESULTS

The periodic rod used in the previous section was machined in bronze using a numerically controlled mechanical lathe. Figure 5 shows a picture of the periodic rod in the experimental setup for FRF measurement. A mini impact hammer was used to impose the excitation at one end, and a mini accelerometer was used to measure the acceleration at the other end. Figure 6 shows the measured FRF superposed with the simulated FRF. A good agreement is found, as expected. The agreement is not perfect due to approximate material properties, geometrical errors in manufacturing and experimental errors. Background noise limits the lower values of the FRF, mainly within the band gap.

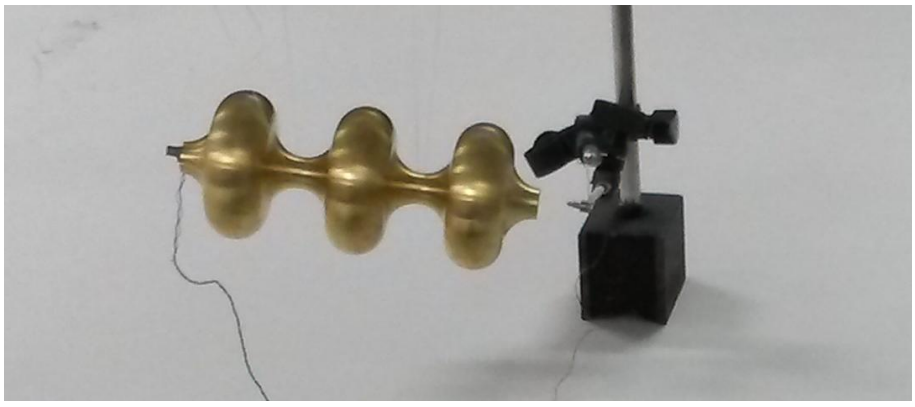

Figure 5: Experimental setup of the impact test used for measuring the FRF of the three-cell rod manufactured in bronze.

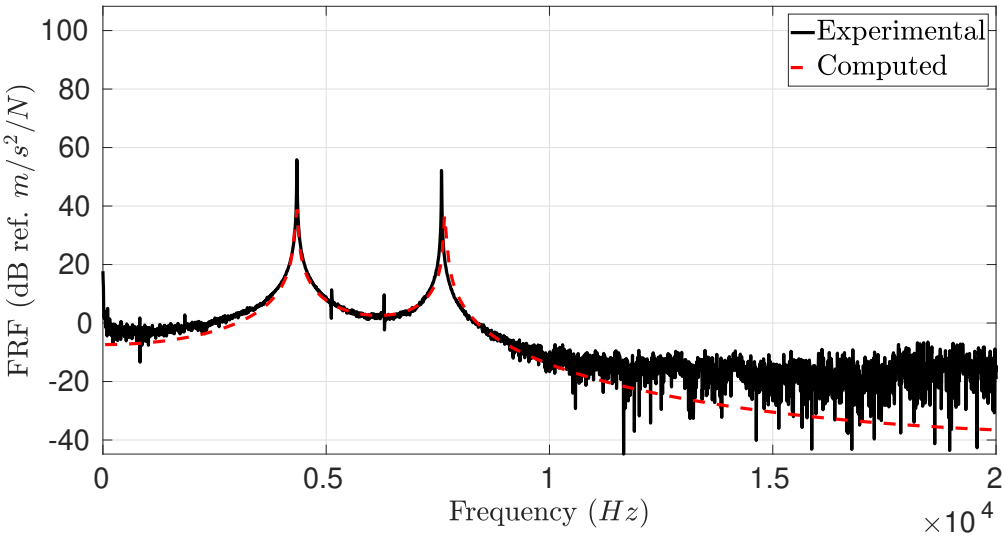

Figure 6: Measured and computed FRFs.

5. CONCLUSIONS

In this work we have formulated and implemented the PWE method for elastic rods with varying cross-sectional area. The method can be used for arbitrarily varying geometrical and material properties that can be expanded in spatial Fourier series. The PWE obtains the dispersion diagram for periodic structures, which show the wave pass bands and stop bands (band gaps). A state-space formulation was used to derive the transfer matrix and the dynamic stiffness matrix of the rod cell. To solve the state-space equations, a transformation of variables leading to a Riccati type equation expressed in terms of the mechanical impedance was performed. With the element dynamic stiffness matrix the forced response of assembled structures with a finite number of cells can be computed. The proposed method has already been extended by the authors to other one-dimensional structures such as acoustic ducts, beams and Levy plates [14].

The semi-analytical solutions exposed in this word can be useful for optimizing the wave behavior and the forced response os one-dimensional structures consisting of a limited number of periodic cells with properties varying along the cell length.

The proposed state-space/Riccati method can be seen as a method to derive spectral elements of one-dimensional structures with arbitrarily varying properties along their length. Such elements can be coupled to assemble a more complex built up structure.

6. ACKNOWLEDGEMENTS

The authors gratefully acknowledge the support of the Brazilian funding agencies CAPES (Finance Code 001), CNPq, FAPESP (Grant Reference Number 2014/19054-6).

7. REFERENCES

[1] M.M. Sigalas and E.N. Economou. Elastic and acoustic wave band structure. *Journal of Sound and Vibration*, 158(2):377 – 382, 1992.

[2] Ming-Hui Lu, Liang Feng, and Yan-Feng Chen. Phononic crystals and acoustic metamaterials. *Materials Today*, 12(12):34 – 42, 2009.

[3] Hasan B. Al Ba'ba'a and Mostafa Nouh. Mechanics of longitudinal and flexural locally resonant elastic metamaterials using a structural power flow approach. *International Journal of Mechanical Sciences*, 122:341 – 354, 2017.

[4] Su Lee, Chang Hoon Ahn, and Jin Woo Lee. Vibro-acoustic metamaterial for longitudinal vibration suppression in a low frequency range. *International Journal of Mechanical Sciences*, 144:223 – 234, 2018.

[5] Mahmoud I Hussein, Michael J Leamy, and Massimo Ruzzene. Dynamics of phononic materials and structures: Historical origins, recent progress, and future outlook. *Applied Mechanics Reviews*, 66(4):040802, 2014.

[6] Mahmoud I Hussein. Reduced bloch mode expansion for periodic media band structure calculations. *Proceedings of the Royal Society A: Mathematical, Physical and Engineering Sciences*, 465(2109):2825–2848, 2009.

[7] Longxiang Xie, Baizhan Xia, Jian Liu, Guoliang Huang, and Jirong Lei. An improved fast plane wave expansion method for topology optimization of phononic crystals. *International Journal of Mechanical Sciences*, 120:171–181, 2017.

[8] J. R. Banerjee and F. W. Williams. Exact bernoulli–euler dynamic stiffness matrix for a range of tapered beams. *International Journal for Numerical Methods in Engineering*, 21(12):2289–2302.

[9] S-K Lee, BR Mace, and MJ Brennan. Wave propagation, reflection and transmission in non-uniform one-dimensional waveguides. *Journal of Sound and Vibration*, 304(1-2):31–49, 2007.

[10] A. MacKinnon and B. Kramer. The scaling theory of electrons in disordered solids: Additional numerical results. *Zeitschrift für Physik B Condensed Matter*, 53(1):1–13, Mar 1983.

[11] G.F.C.A Assis, J.M.C Dos Santos, J.F Camino, and J.R.F. Arruda. Impedance computation using the spectral element method and the riccati equation. *Proceedings of the 2017 CILAMCE*, page 9, 11 2017.

[12] G.F.C.A Assis, E.J.P. Miranda Jr, D. Beli, J.F. Camino, J.M.C. Dos Santos, and J.R.F. Arruda. Computing the dispersion diagram and the forced response of periodic elastic structures using a state-space formulation. *Proceedings of the 2018 ISMA*, 09 2018.

[13] VB Georgiev, J Cuenca, F Gautier, L Simon, and VV Krylov. Damping of structural vibrations in beams and elliptical plates using the acoustic black hole effect. *Journal of sound and vibration*, 330(11):2497–2508, 2011.

[14] G.F.C.A. Assis, D. Beli, E.J.P. Miranda Jr., J.F. Camino, J.M.C. dos Santos, and J.R.F. Arruda. Computing the complex wave and dynamic behavior of one-dimensional phononic systems using a state-space formulation and riccati's equation. *International Journal of Mechanical Sciences (submitted)*, 2019.

[15] J.F. Doyle. *Wave Propagation in Structures: Spectral Analysis Using Fast Discrete Fourier Transforms*. Mechanical Engineering Series. Springer New York, 1997.